OLYMPUS MONS AUREOLE DEPOSITS AND BASAL SCARP: STRUCTURAL CHARACTERISTICS AND IMPLICATIONS FOR FLANK FAILURE SCENARIOS. P. J. McGovern, *Lunar and Planetary Institute, Houston TX 77058-1113, USA (mcgovern@lpi.usra.edu)*, J. R. Smith, *HURL, University of Hawaii, Honolulu, HI, 96822, USA (jrsmith@hawaii.edu)*, J. K. Morgan, *Department of Earth Science, Rice University, Houston, TX 77005, USA (morganj@rice.edu)*, M. Bulmer, *JCET, University of Maryland Baltimore County, Baltimore MD 21227, USA (mbulmer@jcet.umbc.edu).*

Introduction. Olympus Mons is an immense (23 km height above base, 600–800 km wide) volcano located to the northwest of the Tharsis Rise on Mars. The volcanic edifice is partially bounded by an escarpment of height up to 10 km, known as the Olympus Mons basal scarp. Lobate deposits with rugged morphology (the Olympus Mons aureole deposits, abbreviated as OMAD) extend outwards from the base of the scarp for hundreds of kilometers, with greatest extents and widths to the northwest of the edifice. Formation of the OMAD has been attributed to mass movements related to failure of portions of the flanks of Olympus Mons [1–4] or to flows of material (perhaps subsequently eroded) derived and emplaced locally [5–8]. Formation of the basal scarp has been attributed to thrust faulting, [8,9], to the coalescence of mass-movement-related headscarps [1–4], or as a consequence of subglacial volcano growth [11]. While the proximity of scarp segments to aureole lobes is suggestive of a causal relationship, the limited resolution of available datasets has made it difficult to conclusively prove such a link. However, new high-resolution datasets, including Mars Orbiter Laser Altimeter (MOLA) topography [12], offer the potential for vital new insights into the structure and evolution of the Olympus Mons edifice, scarp and aureole. Thus, we examine the structure of the basal scarp and OMAD, as revealed by MOLA topography, from the perspective of evaluation of flank failure scenarios.

Data. We construct topographic cross-sections and slope profiles as a function of distance from the center of the volcano (18.0°N 226.8°E), using a topography grid with 1/128th degree resolution. The profiles fall broadly into two categories: those with a prominent slope break (the basal scarp) and those lacking such a feature. The shallow slopes (generally < 10 degrees) of the central edifice (e.g., Fig. 1) are common to both types. In the profiles lacking a well-defined scarp (e.g., black line in Fig. 1), the lower flanks retain the relatively shallow slopes characteristic of the upper flanks; slopes in excess of 10 degrees are rare or absent. In profiles exhibiting scarps, the peak scarp slopes range from about 20–40 degrees, and the scarps separate gently sloping regions above (flank) and below (smooth materials, probably lava flows, proximal to topographically-rough aureole lobes).

Approach 1: Flank Reconstruction. We apply a flank reconstruction technique [13] to the flank sector due north of the caldera and aureole lobe components Aoam_b and Aoam_c [14], under the assumption that the latter deposits were derived as landslides from the concave, north-facing embayment in the basal scarp. The slide and debris regions were masked out of the original topography and a continuous curvature gridding algorithm was applied using the surrounding topography and a few control points to rebuild the flank and the adjacent plain. The grid tension parameter was adjusted until geomorphologically consistent shapes were reconstructed. Grid subtractions were then performed and the volumes of the missing flank and resulting debris deposit were calculated. The estimated volume for the missing flank is 35×10^3 km^3 with the resulting debris lobe having twice the volume at 70×10^3 km^3, the latter closely matching the Viking era estimate of this deposit [1].

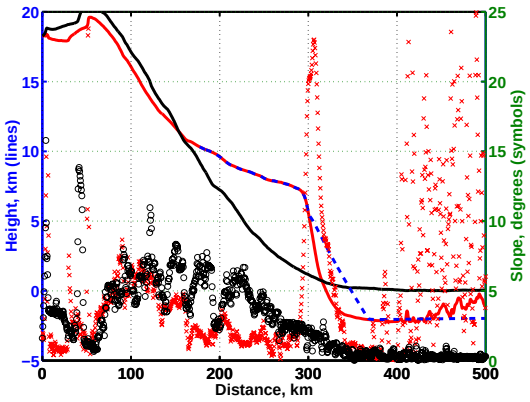

Fig. 1. Topography and slope as functions of distance from the center of Olympus Mons, for profiles with azimuths of 0° (red) and 60° (black). Left vertical axis: observed topography (solid lines), reconstructed flank topography for azimuth 0° profile (blue dashed line). Right vertical axis: observed slopes for azimuth 0° (red 'x') and azimuth 60° (black 'o') profiles.

Approach 2: Flank Failure Modeling. We use Itasca Corporation's Particle Flow Code (PFC2D) [15] to model the dynamics of flank failure. PFC2D, an implementation of the Discrete Element Method (DEM), models discontinuous and heterogeneous deformation via an assemblage of particles subject to Newton's equations of motion, particle interactions with neighboring particles and boundaries, and gravity (see also [16]). A preliminary suite of models was calculated in order to evaluate the effects of basal friction on runout distance. A section of the Olympus Mons flank was modeled by assemblage of particles confined to a parallelpiped 9 km high with slopes of about 30 degrees defining the inner (headscarp) and outer (pre-failure slope) surfaces and with horizontal upper and lower boundaries. To initiate failure, the friction coefficient μ of the basal surface was reduced from the nominal 0.6 to a value in the range 0.0–0.1. For $\mu > 0.06$, the maximum runout distance is less than 100 km, inconsistent with the $>$ 500 km extent of aureole lobe Aoam_b from the basal scarp. In constrast, models with $\mu < 0.04$ yielded runout distances of hundreds of km and flow velocities $v_f > 100$ m/s; such models are consistent with estimates of μ and v_f derived from simple kinematic models constrained by early MOLA data [17].

Discussion. Topographic differences between flank sectors exhibiting scarps and those lacking them have significant implications for studies of scarp and aureole formation processes. For sectors that lack scarps (e.g., black line in Fig. 1), similar slopes are maintained from the caldera rim to the base, suggesting that a uniform process (i.e., construction by effusive basaltic flows) built the topography of the entire flank section. Furthermore the distal regions of non-scarp sectors tend to be covered by relatively smooth, gently-sloped volcanic flows or by relatively old aureole material with subdued relief. Under the assumption of a mass movement scenario, this finding indicates that such sectors of the volcano have been stable since the formation of the old aureole lobes, and that scarps corresponding to such lobes have been buried by the continued emplacement of effusive flows.

For sectors containing scarps (e.g., red line in Fig. 1), slopes just beyond the scarp tend to be very low, probably the result of lava flows from adjoining sectors filling in a topographic low beneath the scarp [14]. However, more distal regions of such sectors tend to be occupied by relatively young and topographically rough aureole lobes. Further, the steepest scarp slopes (northwest sector) are associated with the youngest aureole lobe (Aoau), supporting a scenario in which the scarp is the residual scar from a landslide that created unit Aoau. This sector of the scarp has been least modified by subsequent edifice flows, in contrast to the flow-draped, smoothly sloped sectors lacking scarps (and lobes).

The factor of 2 difference between volume estimates of the reconstructed flank and lobe Aoam has several possible explanations. First, the area of the chosen reconstruction zone may have been too conservative, yielding an underestimate of pre-failure flank extent. Second, the failure surface is probably deeper than accounted for in the model, such that the reconstructed volume underestimates the total volume mobilized by failure. Finally, edifice spreading (below, and [16]) would induce outward flank migration after failure, reducing the reconstructed volume. Further development of the technique will address these issues. However, slopes of the reconstructed flank sector facing the north Aoam lobes (Fig. 1, blue dashed line) are similar to lower flank slopes of the flow-constructed, escarpment-lacking sectors, (Fig. 1, black line) suggesting that the latter type of sectors are capable of producing scarp- and aureole-forming events.

Mechanisms that could generate scarp and aureole structures via flank failure fall into several categories. We first consider edifice spreading or thrusting. In such models, the Olympus Mons basal scarp is an expression of thrust faulting at edge of the edifice. For example, [9] proposed that the scarp was exposed face of an anticline generated by deeply-rooted failure of the crust beneath the edifice, analogous to structures seen on the flanks of spreading central american volcanoes. However, the extremely thick mechanical lithosphere supporting Olympus Mons [18] makes it difficult to generate horizontal compressive stresses of the required magnitude. Further, such a model does not explicitly address the association with aureole deposits. However, spreading scenarios that posit a pre-existing plane of weakness are feasible. For example, recently discovered thrust ramp structures, rooted in a basal detachment, on the submerged flanks of the Kilauea and Mauna Loa volcanoes [19], can generate landslide deposits that initiate from oversteepened thrust ramps. Such a scenario shares some attributes of the second class of models (described below) and can explain the association of the basal scarp with aureole lobes [16].

An alternative class of models generates scarp and aureole featues by extensional failure: i.e., as the coalesced headscarps of large landslides [1–4, 20]. Such models also invoke weak basal layers or decollements [4]. A Hawaiian-style basal detachment model for Olympus Mons [4,20] requires that buildup of pore water overpressure in a low permeability layer would reduce effective fricton [21], facilitating outer flank spreading [20]. However, high lithostatic pressures beneath central edifice would close pore spaces, yielding a welded edifice/lithosphere boundary [20]. The latter boundary condition [4] is consistent with the absence of mid-flank graben and the presence of mid-flank ridges that may indicate compression [Tea 90]. Under such a model, the radial extent of scarp would indicate transition between dry (no slip) and wet (decollement) basal layers [22]. Furthermore, local conditions (presence of pore fluid or low-permeability substrate, or boundary roughness [23]) may dictate the likelihood of failure and thus the presence or absence of basal scarp and aureole structures within a given sector. The requirement of pore fluid for detachment behavior implies the presence of liquid water, an inference supported by the high incidence of water-activated slope streaks in the OMAD region [24]. Given the extreme youth of such features, ongoing fluid-enabled flank failure at Olympus Mons is possible.

References. [1] R. M. Lopes *et al.*, *JGR, 87*, 9917, 1982. [2] P. W. Francis and G. Wadge *JGR, 88*, 9333, 1983. [3] K. L. Tanaka, *Icarus, 62*, 191, 1985. [4] P. J. McGovern and S. C. Solomon, *JGR, 98*, 23,553, 1993. [5] E. C. Morris, *JGR, 87*, 1164, 1982. [6] M. H. Carr, *JGR, 78*, 4049, 1973. [7] J. S. King and J. R. Riehle, *Icarus, 23*, 300, 1974. [8] E. C. Morris and S. E. Dwornik, *USGS Map I-1049*, 1978. [9] A. Borgia et al. *JGR, 95*, 14,357, 1990. [10] C. A. Hodges and H. J. Moore, *JGR, 84*, 8061,1979. [11] J. Helgason, *Geology, 27*, 231, 1999. [12] D. E. Smith *et al.*, *JGR, 106*, 23,689, 2001. [13] K. Satake *et al.*, *Hawaiian Volcanoes: Deep Underwater Perspectives, Geophysical Monograph 128*, 333, AGU, Washington, DC, 2002. [14] E. C. Morris and K. L. Tanaka, USGS map I-2327, 1994. [15] Itasca Consulting Group, *PFC2D Users Guide*, Itasca Consulting Group, Minneapolis, 1999. [16] J. K. Morgan and P. J. McGovern, this volume, 2003. [17] M. H. Bulmer and P. J. McGovern *LPS, 30*, abstract 2016, 1999. [18] P. J. McGovern *et al.*, *JGR, 107*, 10.1029/2002JE001854, 2002. [19] J. K. Morgan *et al.*, *Geology, 28*, 667, 2000. [20] P. J. McGovern and S. C. Solomon, *LPS, 28*, abstract 1731, 1997. [21] R. M. Iverson, *J. Volcanol. Geotherm. Res., 66*, 295, 1995. Future directions. [22] P. J. Thomas *et al.*, *JGR, 95*, 14,345, 1990. [23] P. J. McGovern, Ph.D. thesis, M.I.T., 339 pp., 1996. [24] N. Schorghofer *et al.*, *GRL, 29*, doi 10.1029/2002GL015889, 2002.